BLIND IMAGE QUALITY ASSESSMENT IN THE COMPLEX FREQUENCY DOMAIN

Kais Rouis[1,3]*, Mohamed-Chaker Larabi*[2]*, Jamel Belhadj Tahar*[3]

[1] National School of Engineering of Tunis, University of Tunis El Manar, Tunisia
[2] XLIM Laboratory, CNRS, University of Poitiers, France
[3] Innov'COM Laboratory, Sup'Com, University of Carthage, Tunisia

ABSTRACT

In this paper, we propose a no-reference (NR) image quality assessment (IQA) metric that operates in the complex frequency domain. A set of features are developed to model the natural scene statistics without depending on any specific visual distortion. The proposed approach relies on a statistical analysis of the transformed image, involving the importance of the phase and magnitude provided by the underlying complex coefficients. We further investigate the correlation between the different image spatial-frequency resolutions, i.e., representations under different scales and orientations in order to extract the directional features and energy distributions of an image. The validation of the NR metric is performed on a variety of challenging IQA databases and the obtained results show good correlation with subjective scores. Besides, the obtained performance is highly competitive compared to the top-performing NR IQA metrics.

Index Terms— No-reference IQA, complex frequency domain, relative phase and magnitude.

1. INTRODUCTION

The increased need of assessing the quality of visual signals is typically linked to the expansive area of image and video transmission, along with the extended capabilities of connected devices such as (ultra) high definition televisions (HDTV/UHD), Internet video streaming and so on. The end-user's quality of experience (QoE) in such communication systems is therefore a main constraint to approve the feasibility when handling visual data. Most of the operations introduce distortions to the original visual information with variable annoyance levels. On the other hand, in order to guarantee a satisfactory QoE, a significant network bandwidth consumption is often required [1]. Formally, image quality assessment (IQA) in multimedia services becomes a primary topic, as it could further be adapted to standard compression schemes, to judge or even monitor the implemented process based on a visual quality assessment module. The objective is therefore to provide an adequate QoE using objective measures of visual quality, which is often qualified as a perceptual approach.

Several IQA algorithms have been proposed to provide an objective image quality assessment and could be categorized as full reference (FR), reduced reference (RR), or no-reference (NR) metrics. The latter classification depends on the proportion of the reference image involved in the estimation of the associated distortions. The literature related to FR metrics is very rich and several interesting surveys have been performed. This is far from being the case of NR quality metrics even though some very interesting works have been proposed [2–6]. The focus of this work is on NR IQA and precisely on algorithms following the hypothesis that natural world images occupy a small subspace of the space of all possible images, including the distorted ones. This would bring us to seek a reliable generalization of natural images based on an expanded statistical modeling supplying accurate image features [7]. For instance, a Bayesian inference model has been proposed to extract features based on image DCT coefficients. The parameters of this model are estimated to predict the quality score [3]. In [4], the features are captured in the spatial domain from empirical and local distribution of normalized luminance. The correlation of the predicted scores with subjective judgment is highly competitive compared to other approaches. The statistics of complex wavelet coefficients were inspected using the wrapped Cauchy model and the generalized Gaussian distribution distribution (GGD) to explore the relationships between corresponding magnitudes and phases [6]. Actually, we consider this work to assess the proposed framework as we adopt the complex domain for image features' extraction. Furthermore, images were transformed in the curvelet domain with the aim to extract the statistical features based on the log-histograms of the curvelet coefficients, and an asymmetric generalized Gaussian distribution model [5]. Besides the authors included the energy orientation distributions for predicting the quality.

We rely on transforms to the frequency domain in order to get robust and accurate image descriptors [8]. In comparison to the method in [5], we use a convenient discrete version of the curvelet transform namely, the uniform discrete curvelet transform (UDCT) [9], which provides a set of directional complex subbands along different frequency resolutions. The adopted framework of this frequency analysis in the complex domain, offers several properties such as the shift invariance in the energy sense and a lower redundancy over existing transforms. Further additional properties make the UDCT very effective and practical for offering a good plan of quality measurement. Particularly, the transform is well adapted to fine information, representing features like edges, shapes, etc. These features are tied to human perception and the fact of building our metric on such features will allow to account for perceptual aspects, leading thus to a correlation with human judgment of quality. Even though statistical modeling of the provided complex coefficients could be an effective tool for an adequate signal estimation, performing the required estimation process is not evidently and directly achievable especially, if we aim to propose an effective generic framework of quality measurement. In other words, performing an estimation method to fit the empiric data based on accurate parameters, or exploiting directly the provided information is related to several constraints of which the performance is the major one.

The aim of this work is to prove the feasibility of the evaluation approach through an effective exploitation of visual aspects. The main interest is to obtain a convincing accuracy independently of the change of typical distortions or datasets. One more tendency is to concern the ability of exploring the assessment efficiency of accurate features in different image block-based processing scheme,

which could be beneficial for a perceptual optimization strategy. This would be achieved while not depending on a process that requires a sophisticated training method to amplify the effect of quality descriptors. In this paper, we will demonstrate the effectiveness of the proposed quality metric based on a uniform representation in the frequency domain. The metric is founded by certain complementary features to predict the final score, subsequently to a regression model similar to the compared IQA algorithms.

The rest of the paper is organized as follows. In Section 2, we describe the proposed image quality assessment features corresponding to the proposed relative phase and magnitude (RPM) metric. Section 3 presents the performed experiments on different IQA databases, to show how RPM correlates with human opinions of visual quality. Finally, some conclusions are drawn in the last section.

2. PROPOSED QUALITY MEASUREMENT

Creating an effective IQA metric is proportional to image features catching as much as possible the contained information. Indeed, these features should be sufficient enough to identify the degree of distortions independently from the image content. First, we divide a given image into blocks of size 32×32 making the use of extracted information more flexible relative to other block-based applications, and it is quite enough for our work as presented visual details. Then, each block is transformed into the frequency domain using the UDCT form; two scales of resolutions 16×16 and 8×8, representing the fine and the coarse scales, respectively. Within each scale, we use six orientations and as a result, we obtain 12 matrices corresponding to the provided complex subbands. It is worth mentioning that the whole set of features of each image is calculated as the average of the blocks' features, even when combinations between the different scales/orientations are performed.

2.1. Phase-based Measure

Multi-scale Extraction

The phase information can be captured based on the directional features within the complex subbands.We need therefore to elaborate the convenient phase relationships, in order to accurately reflect local edges. As stated in [10], the phases change linearly with the distance to the surrounding step or ramp in a directional subband. This interesting statement was later proved to generalize the phase linearity to different complex transformation domains. Starting from a unit step signal and ideal complex filter $H(\omega) = 1$ if $0 \leq \omega_1 \leq \omega \leq \omega_2$, the phase could be approximated as [11]:

$$y_{step}(r) \simeq \left(\frac{\omega_2 - \omega_1}{\ln \left| \frac{\omega_2}{\omega_1} \right|} \right) r - \frac{\pi}{2}, \quad y_{ramp}(r) \simeq \left(\frac{\omega_1 \omega_2 \ln \left| \frac{\omega_2}{\omega_1} \right|}{\omega_2 - \omega_1} \right) r.$$

These approximations describe the proportional linearity relationship between local phase and distance r with the orientation feature *step* or *ramp*. We benefit from this property to capture phases' behavior within each subband based on a specific coefficients' relationship. The distance will be evidently considered as the relative phase (RP) between the coefficients as follows:

$$p_{s,\theta}(i,j) = \begin{cases} \angle c_{s,\theta}(i,j) - \angle c_{s,\theta}(i,j+1) \; if \; 1 \leq \theta \leq \dfrac{K}{2}, \\ \angle c_{s,\theta}(i,j) - \angle c_{s,\theta}(i+1,j) \; if \; \dfrac{K}{2} < \theta \leq K. \end{cases} \quad (1)$$

where $\angle c_{s,\theta}(i,j)$, with $s = 1,..,S$ and $\theta = 1,..,K$ ($S = 2$ and $K = 6$), is the angle of the complex coefficient at location (i,j) within a matrix subband of scale s and orientation θ. The shape of the RPs is similar to the Gaussian distribution so it would be meaningful to explore it. Actually, we have a matrix for each directional subband representing a non-uniform distribution owning more useful statistical behaviour. The following features are extracted based on these provided matrices instead of the original complex subbands.

The usual statistics that can be applied to the magnitudes for instance, cannot be evidently used with such circular data. Circular statistics concern samples' realizations of random variables that are circularly distributed. In fact, the underlying trigonometric moments are defined in terms of density functions through which we could describe several characteristics, as the peakedness in the circular density and its variance. These kind of statistics provide the estimates of theoretical values from the given samples. Let $\phi = \{\alpha_i\}$ the set of N angles in the range of $[-\pi, \pi]$. The first-order trigonometric moment of ϕ is given by:

$$\phi_1 = \frac{1}{N} \sum_{i=1}^{N} e^{j\alpha_i}, \quad (2)$$

The obtained complex number ϕ_1 can be interpreted as the sum of N unit vector angles in ϕ. This latter is considered as the set of angles in the matrix $p_{s,\theta}$ representing the relative phases within a directional subband, lying in the complex plain of the transform *coarsest scale*. We propose afterward the *mean direction* $\overline{\alpha}$, the angle $\angle\phi_1$, as a measure of the mean direction.

We would indeed describe the data samples from higher trigonometric moment order, but this time using the *finest scale* which is rich of finer information and can be deterministic to capture distortion of main visual patterns. Because of this, we calculate the *circular kurtosis* as follows, which supplies coefficients at every angle that are normalized with regard to the cyclic energy, and allows detecting angular positions where the kurtosis takes high or low values

$$k_\theta = \frac{1}{N} \sum_{i=1}^{N} \cos[2(\alpha_i - \overline{\alpha})]. \quad (3)$$

where α_i is the angle in the RP matrix $p_{s,\theta}$ and $\overline{\alpha}$ is the circular mean of N analogous circular directions.

The chosen definition is appealing, since many values close to the mean direction lead to positive contributions to the above average, due to the shape of the cosine function [12]. The measure is therefore appropriate to explore the information without a requirement of other form which is related to circular analogues of some distribution function. Till now, the two features are measured separately over two different scales, where each one is performed to the six orientations along a scale.

Inter-scale Extraction

The correlation between coefficients of the fine and coarse scales can be further used to improve the performance of the signal estimation at multi-scale features [13]. The inter-scale phase relationship is captured as follows:

$$p_{r,\theta} = \angle c_{s,\theta}(i,j) - 2\angle c_{s+1,\theta}(i',j'). \quad (4)$$

The resulting matrix $p_{r,\theta}$ in Eq. 4 is a product of the phase coefficients within two subbands of the same orientation θ, (i,j) represents the location of the parent coefficient and (i',j') is the equivalent coefficient in the finest scale. We apply on $p_{r,\theta}$ the RP as in Eq. 1 to take profit from the obtained angular distribution. The *mean direction* is

then calculated over the provided matrices using the same formula as described above. Besides, we calculate the *circular variance* to measure the spread of the circular data samples' density defined by $1 - |\phi_1|$, where $|\phi_1|$ is the magnitude of the resulted complex number ϕ_1 in Eq. 2. The circular variance is quietly robust to indicate the amount orientation selectively which would have strong effect in this context. Therefore, we have two additional phase features that represent the inter-scale phase relationship based on two moment orders. Each one is computed over a provided matrix $p_{r,\theta}$ between the two scales, corresponding to six different directions.

2.2. Magnitude-based Measure

Multi-scale Extraction

The energy is a primordial feature for representing the sensitivity factor of human perception within the cortical neurons. Implicit characteristics such as the good directional selectivity drove us to describe the unnatural distortions using the *log-energy*. This measure is obtained in order to capture the local spectral signatures of a particular subband (Eq. 5), as the applied transformation afford a set of complex subbands' coefficients which are rich of information But first, an intra-subband transformation is designed as the difference between the magnitude of adjacent complex coefficients. This transformation is called in the following as the relative magnitude (RM) which is given for one subband as proposed for the RP in Eq. 1, depending evidently of mostly horizontal or vertical directional subbdands. A matrix $m_{s,\theta}$ is therefore provided over a scale $s = \{1, 2\}$, while representing one direction $\theta = \{1, .., 6\}$. The benefit of such an operation is to represent a certain dependability across spatial locations, and consider the spectral dissimilarities to exploit the frequency levels throughout the harmony of higher and lower radial spatial frequencies.

$$El_{s,\theta} = \log\left(1 + \frac{1}{N}\sum_{i=1}^{N} |c_{s,\theta}(i, j)|^2\right), \tag{5}$$

where $|c_{s,\theta}(i, j)|$ is the magnitude of complex coefficient at a location (i, j) within $m_{s,\theta}$.

We choose to consider the *coarsest scale* as a first magnitude based energy feature, as it is rich of basic visual information. As we are treating two scales, it is reasonable to efficiently take profit from disparity in the energy between different resolution levels. Indeed, we take secondly the ratio between the corresponding energies as follows

$$El_n = \frac{|El_{s,\theta} - El_{s+1,\theta}|}{El_{s,\theta} + El_{s+1,\theta}}, \qquad n = \{1, .., 6\}. \tag{6}$$

where $El_{s,\theta}$ represents the log-energy of a subband with orientation θ and scale s.

Besides, another aspect has been considered in our work which takes into account the distribution of energy according to its median:

$$Ed_{s,\theta} = \frac{\sigma(m_{s,\theta})}{\mu(m_{s,\theta})}, \tag{7}$$

For the feature $Ed_{s,\theta}$, extracted from each provided subband, the spread of the coefficient magnitudes (numerator) is mediated by the effect of actual matrix's center (denominator), of which the variation of coefficients that indicate the energy orientation, is typically emphasized for correlating visual impressions. Based on this measure, we implicate further the distortion variance between higher and lower frequencies, to capture the multi-scale energy correlation, which is given as follows

$$Ed_n = Ed_{\theta_n,s} - Ed_{\theta_n,s+1}. \tag{8}$$

where Ed_n ($n = \{1, .., 6\}$) is the difference between energies of analogous subbands, while having the same orientation within two given scales, and based on the formula shown in Eq. 7.

Inter-scale Extraction

It is obvious that an image pattern is presented over different resolutions in such a way the corresponding coefficients are highly correlated. This concept has been proved in the context of multi-scale matching upon complex wavelets, in order to define the nature of multilevel features [10]. In order to identify ridges against step edges, looking for information across scales should have a valuable impact. We use the product of magnitudes between subband orientations at two adjacent scales to disclose the underlying importance of these features. We recall that the coefficients maintain shift-invariance property, and therefore a reliable estimation of rich information is maintained across the fine and coarse scales.

$$m_{r,\theta} = |c_{s,\theta_n}(i, j)| * |c_{s+1,\theta_n}(i', j')|. \tag{9}$$

The UDCT as a curvelet discrete version offers the parent-child relationship between coefficients, which is employed to perform the inter level product. The uniform compact frequency support of curvelet basis functions is accordingly another key for employing this transformation. The resulting matrix $m_{r,\theta}$ in Eq. 9 is a product of the magnitude coefficients within two subbands of the same orientation θ, (i, j) represents the location of the parent coefficient and (i', j') is the equivalent coefficient in the finest scale. We adopt the same policy; suitable theoretical settlement with a straight and explicit estimate of information. We performed the same measure from Eq. 7 in this sens from the new six produced magnitude matrices.

2.3. Quality Measurement

To summarize, we implemented a set of features in the UDCT complex domain from two main sources; the phase and magnitude. For phase-based measures, we computed the circular mean from the coarse scale and the circular kurtosis from the finer scale as two trigonometric orders. Besides, the circular mean was moreover explored from a new generated (by Eq. 4) set of six matrices, along with the circular variance.

The magnitude-based measures were extracted using the log-energy of subbands in the coarse scale in addition to correlation energies across scales from Eq. 6, and the relative energy distribution of each directional subband again in addition to correlation energies across scales from Eq. 8. Finally the feature in Eq. 7 is moreover calculated over the set of six generated matrices (by Eq. 9).

A mapping is therefore performed from the features space to image quality prediction scores. A support vector machine regressor (SVR) is set up given that is widely applied in this topic and effective for handling high dimensional data [14]. Since the performance evaluation requires a step of features mapping, each considered image database is divided into randomly chosen training set and testing set such that both sets were absolutely separated by content. The package in [15] is utilized to implement the ϵ-SVR with a radial basis function (RBF) kernel regression. The training-testing procedure is repeated 1000 times in order to avoid the case of performance bias. The Spearman's rank ordered correlation coefficient (SROCC) and Pearson's linear correlation coefficient (LCC) between the predicted scores from the algorithms and subjective scores, are used as

performance indicators and the median across the 1000 iterations is finally reported.

3. EXPERIMENTS AND RESULTS

To benchmark our IQA metric, we used the popular *LIVE IQA database* [16] which contains 29 reference images and 779 distorted images, impaired by different levels of five distortion categories: JPEG 2000 (JP2K), JPEG, additive white noise (WN), Gaussian blur (Blur), and a Rayleigh fast-fading channel (FF) simulation. An associated realigned human differential mean opinion scores (DMOS) [17] is further available to represent the perceived quality of the images. We utilized as well the *Live in the Wild image quality challenge database*, which is considered as a difficult resource and contains 1162 images that are authentically distorted and captured from a variety of modern mobile devices [18]. Moreover, we considered the *TID2013 database* [19] introducing various severe distortions (24 types); which makes it very interesting from a practical viewpoint, with 3000 distorted versions of 25 reference images. We note that the tests are performed on 24 images excluding one synthetic reference and its associated images.

In fact, we evaluated our metric against five interesting No-Reference approaches: C-DIIVINE [6], BRISQUE [4] and CurveletQA [5]. We note here that C-DIIVINE is an extension of DIIVINE [2] in the complex domain and provided a superior performance, and the same case for BRISQUE and CurveletQA that proved a particular performance compared to preceding IQA algorithms such as BIQI [20] and BLIINDS-II [3]. The NR IQA algorithm performance is ensured by the strength of features to identify the image distortions. The features must be complementary to each other in such a way the framework would be generic, independently from any use of regression methods. Therefore to insure fair experiments, we used the same score's prediction model (subsection 2.3) for all compared approaches and the performance was obtained from the same selected train-test datasets.

Table 1: Performance across 1000 train-test combinations on the LIVE IQA database.

	Median	*SROCC*				
	JP2K	JPEG	WN	Blur	FF	ALL
BRISQUE	0.9118	0.9245	0.9709	0.9544	0.8835	0.9284
CurveletQA	0.9285	0.9387	**0.9791**	0.9569	0.8864	0.9329
C-DIIVINE	**0.93394**	0.9376	0.9623	0.9620	**0.9075**	0.9390
RPM	0.9293	**0.9524**	0.9769	**0.9686**	0.8986	**0.9491**
	Median	*LCC*				
	JP2K	JPEG	WN	Blur	FF	ALL
BRISQUE	0.9187	0.9607	0.9764	0.9573	0.9083	0.9341
CurveletQA	0.9420	0.9628	**0.9845**	0.9535	0.9002	0.9374
C-DIIVINE	**0.9468**	0.9554	0.9670	0.9501	**0.9201**	0.9433
RPM	0.9398	**0.9748**	0.9787	**0.9682**	0.9153	**0.9521**

Table 2: Performance across 1000 train-test combinations on the TID2013 and LIVE in the Wild IQA databases.

TID2013		
	SROCC	LCC
CurveletQA	0.5010	0.5896
BRISQUE	0.5984	0.6695
C-DIIVINE	0.6260	0.6926
RPM	**0.7104**	**0.7620**

Live in the Wild		
	SROCC	LCC
CurveletQA	0.6124	0.6197
BRISQUE	0.5843	0.6068
C-DIIVINE	0.6485	0.6660
RPM	**0.6533**	0.6623

All NR algorithms' performance are provided in Table 1 and 2, obtained by the same 80% training - 20% testing samples over 1000 iterations. From the shown results, we can see that the proposed RPM is statistically superior considering the LCC and SROCC indices for the overall tested databases. The metric evinced a competitive behavior for each distortion type for the Live database, and the correlations are very convincing. The same applies for the Live in the Wild which represents a particular challenge compared to standard legacy databases, seeing that is not based on a set of impairment levels for each reference image. For this database, our metric and that of C-DIIVINE provide better correlations than BRISQUE and CurveletQA with similar LCC index and more better SROCC index for RPM. Furthermore, RPM has proved a particular efficiency and significant higher indices on the TID2013, taking into account the severe distortions presented in this database and the huge variety of evaluated samples.

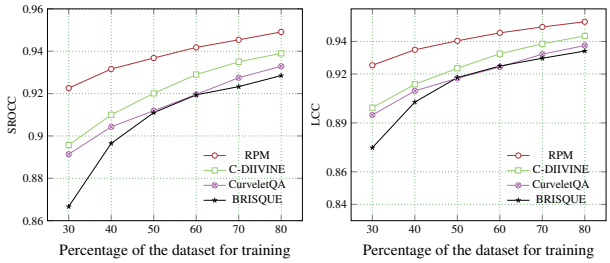

Fig. 1: Plot of median SROCC (a) and LCC (b) between predicted and subjective DMOS scores (on all LIVE IQA databse) as a function of the percentage of the dataset used for training.

The dependency of IQA algorithms to the training subset is a limitation that should be inspected. In order to investigate the prospect of the relevant features, we varied the percentage of the train dataset from 30% to 80% of the content and the remaining of each proportion is used as the test dataset. As shown in Figure 1, the performance of RPM on Live database is better than the other methods for all percentages, and is consistently above 0.92 even using a 30% of train dataset. This consistent performance confirms that our proposed features characterize effectively the analyzed signal, although compared to C-DIIVINE similarly based on the complex domain. This could be endorsed even if we compare RPM with the CurveletQA metric which uses alike transformation.

4. CONCLUSION

We described a novel model for the No-Reference image quality assessment task. The quality measure is based on a set of accurate features extracted from the image complex frequency representation. These features were extracted using the coefficients' magnitude and phase information. The efficiency was accordingly demonstrated using three publicly available databases that represent different characteristics and distortion types. One of the three databases (Live in the wild) is atypical and very challenging for the quality assessment community. The superior performance over the compared approaches without requiring a large train dataset, along with the high correlation with human visual judgments, make us believe that this model may be exploited in an extended perceptual analysis and compression scheme.

5. REFERENCES

[1] Alan C Bovik, *Handbook of image and video processing*, Academic press, 2010.

[2] Anush Krishna Moorthy and Alan Conrad Bovik, "Blind image quality assessment: From natural scene statistics to perceptual quality," *IEEE Transactions on Image Processing*, vol. 20, no. 12, pp. 3350–3364, 2011.

[3] Michele A Saad, Alan C Bovik, and Christophe Charrier, "Blind image quality assessment: A natural scene statistics approach in the dct domain," *IEEE Transactions on Image Processing*, vol. 21, no. 8, pp. 3339–3352, 2012.

[4] Anish Mittal, Anush Krishna Moorthy, and Alan Conrad Bovik, "No-reference image quality assessment in the spatial domain," *IEEE Transactions on Image Processing*, vol. 21, no. 12, pp. 4695–4708, 2012.

[5] Lixiong Liu, Hongping Dong, Hua Huang, and Alan C Bovik, "No-reference image quality assessment in curvelet domain," *Signal Processing: Image Communication*, vol. 29, no. 4, pp. 494–505, 2014.

[6] Yi Zhang, Anush K Moorthy, Damon M Chandler, and Alan C Bovik, "C-diivine: No-reference image quality assessment based on local magnitude and phase statistics of natural scenes," *Signal Processing: Image Communication*, vol. 29, no. 7, pp. 725–747, 2014.

[7] Tomás Brandão and Maria Paula Queluz, "No-reference image quality assessment based on dct domain statistics," *Signal Processing*, vol. 88, no. 4, pp. 822–833, 2008.

[8] Kais Rouis, Sami Jaballah, Faten Ben Abdallah, and Jamal Bel Hadj Tahar, "Udct complex coefficient statistics based rotation invariant texture characterization," in *Visual Communications and Image Processing Conference, 2014 IEEE*. IEEE, 2014, pp. 430–433.

[9] Truong T Nguyen and Hervé Chauris, "Uniform discrete curvelet transform," *IEEE Transactions on Signal Processing*, vol. 58, no. 7, pp. 3618–3634, 2010.

[10] Ryan Anderson, Nick Kingsbury, and Julien Fauqueur, "Coarse-level object recognition using interlevel products of complex wavelets," in *IEEE International Conference on Image Processing 2005*. IEEE, 2005, vol. 1, pp. I–745.

[11] An Vo and Soontorn Oraintara, "A study of relative phase in complex wavelet domain: Property, statistics and applications in texture image retrieval and segmentation," *Signal Processing: Image Communication*, vol. 25, no. 1, pp. 28–46, 2010.

[12] Arthur Pewsey, "The large-sample joint distribution of key circular statistics," *Metrika*, vol. 60, no. 1, pp. 25–32, 2004.

[13] Mark Miller and Nick Kingsbury, "Image modeling using interscale phase properties of complex wavelet coefficients," *IEEE Transactions on Image Processing*, vol. 17, no. 9, pp. 1491–1499, 2008.

[14] Christopher JC Burges, "A tutorial on support vector machines for pattern recognition," *Data mining and knowledge discovery*, vol. 2, no. 2, pp. 121–167, 1998.

[15] Alexandros Karatzoglou, Alex Smola, Kurt Hornik, and Achim Zeileis, "kernlab-an s4 package for kernel methods in r," 2004.

[16] L. Cormack A.C. Bovik H.R. Sheikh, Z. Wang, "Live image quality assessment database release 2," http://live.ece.utexas.edu/research/quality.

[17] Hamid R Sheikh, Muhammad F Sabir, and Alan C Bovik, "A statistical evaluation of recent full reference image quality assessment algorithms," *IEEE Transactions on image processing*, vol. 15, no. 11, pp. 3440–3451, 2006.

[18] Deepti Ghadiyaram and Alan C Bovik, "Massive online crowdsourced study of subjective and objective picture quality," *IEEE Transactions on Image Processing*, vol. 25, no. 1, pp. 372–387, 2016.

[19] Nikolay Ponomarenko, Oleg Ieremeiev, Vladimir Lukin, Karen Egiazarian, Lina Jin, Jaakko Astola, Benoit Vozel, Kacem Chehdi, Marco Carli, Federica Battisti, et al., "Color image database tid2013: Peculiarities and preliminary results," in *Visual Information Processing (EUVIP), 2013 4th European Workshop on*. IEEE, 2013, pp. 106–111.

[20] Anush Krishna Moorthy and Alan Conrad Bovik, "A two-step framework for constructing blind image quality indices," *IEEE Signal Processing Letters*, vol. 17, no. 5, pp. 513–516, 2010.